Low-Temperature Compounding of Flax Fibers with Polyamide 6 via Solid-State Shear Pulverization (SSSP): Towards Viable Natural Fiber Composites with Engineering Thermoplastics

Journal:	*Polymer Composites*
Manuscript ID	PC-18-1157.R2
Wiley - Manuscript type:	Research Article
Date Submitted by the Author:	n/a
Complete List of Authors:	Wakabayashi, Katsuyuki; Bucknell University, Department of Chemical Engineering; KU Leuven, Department of Materials Engineering, Group T Leuven Campus, Andreas Vesaliusstraat 13 Assfaw, Mekdes; KU Leuven, Department of Electromechanical Engineering, Group T Leuven Campus, Andreas Vesaliusstraat 13 Vancoillie, Simon; KU Leuven, Department of Electromechanical Engineering, Group T Leuven Campus, Andreas Vesaliusstraat 13 Choi, David; Bucknell University, Department of Chemical Engineering Desplentere, Frederik; KU Leuven, Department of Materials Engineering, Bruges Campus, Spoorwegstraat 12 van Vuure, Aart; KU Leuven, Department of Materials Engineering, Group T Leuven Campus, Andreas Vesaliusstraat 13
Keywords:	compounding, flax, polyamide, thermoplastics, solid-state shear pulverization

Low-Temperature Compounding of Flax Fibers with Polyamide 6 via Solid-State Shear Pulverization (SSSP): Towards Viable Natural Fiber Composites with Engineering Thermoplastics

Katsuyuki Wakabayashi*[1,2], Simon H.E. Vancoillie[3], Mekdes G. Assfaw[3], David H. Choi[1], Frederik Desplentere[2,4], and Aart W. Van Vuure[2,5]

[1] Bucknell University, Department of Chemical Engineering, Lewisburg, PA 17837, U.S.A.

[2] Katholieke Universiteit Leuven, Department of Materials Engineering, Composite Materials Group, Leuven 3001, Belgium

[3] Katholieke Universiteit Leuven Campus Group T, Department of Electromechanical Engineering Technology, Leuven 3000, Belgium

[4] Katholieke Universiteit Leuven, Bruges Campus, Processing of Polymers & Innovative Materials Group, Bruges 8200, Belgium

[5] Katholieke Universiteit Leuven, Campus Group T, Department of Chemical Engineering Technology, Leuven 3000, Belgium

* Corresponding Author

Submitted as an original article to *Polymer Composites*

ABSTRACT

Low-temperature compounding of natural fiber/thermoplastic composites via solid-state shear pulverization (SSSP) is explored for the first time, with a goal of processing temperature-sensitive natural fibers with high temperature-melting engineering thermoplastics without fiber degradation. The model study was based on polyamide 6 (PA6) as the matrix material and short flax fibers as the filler materials; flax fiber type was varied to provide a range of comparison. Composite structural characterization was conducted using computer tomography, optical microscopy, and scanning electron microscopy, while mechanical property measurements were performed on injection molded specimens in both tension and bending. SSSP demonstrated robust and effective processing results in model PA6/flax composites, especially when compared to conventional extrusion. SSSP was able to isolate unmodified scutched fibers into individual elementary fibers with minimal scission, and effectively distribute them in the polymer matrix in situ. The dispersed and distributed filler morphology led to mechanical property enhancements, including 230% and 40% increases in Young's modulus and tensile strength, respectively, compared to neat PA6, at a 20 vol% fiber content.

KEYWORDS

Compounding, Flax, Polyamide, Thermoplastics, Solid-state shear pulverization.

INTRODUCTION

While glass and carbon fibers continue to be predominantly used in today's composite applications due to their established mechanical properties for the respective densities and costs [1,2], global sustainability efforts have generated growing interests in developing environmentally friendly, renewable filler materials for green, bio-based composites. A highly viable option are fibers derived from natural plant components (natural fibers), which have environmental benefits such as sustainable production, CO_2 neutrality, and minimal energy embodiment [3-6]. Natural fibers can contribute additional, often unique, combinations of optical, haptic, and acoustic/vibrational damping properties, as well as practical advantages like low density, low cost, and low wear to processing equipment and tooling [4,7-10].

The range of applications for natural fiber composites is expanding beyond niche markets like furniture and leisure into major manufacturing sectors such as automotive, structural, and packaging [4,11-14]. In such arenas of large-scale production, thermoplastics-based composites containing short discontinuous fibers are often melt-compounded using a twin screw extruder (TSE) [15-17] prior to being molded into final forms. Though this established, commercially applicable process has been successful with natural fibers to certain extent [18-28], melt-compounding of natural fibers with plastics has several challenges. One inherent issue of natural fibers is their relatively low thermal degradation/decomposition temperatures (T_{deg}) [29,30], along with their hygroscopicity [31,32]. Accordingly, previous reports of melt-compounding of natural fibers in plastics have been mainly restricted to low-glass transition temperature (T_g) or low-melting temperature (T_m) polymers [33], such as polypropylene (PP) [19-23], polyethylene (PE) [24-26], and polylactic acid (PLA) [27,28].

Another challenge is the complex morphological hierarchy of natural fibers' structural components, whose respective properties depend on the mechanical preparation processes such as breaking, scutching and hackling, as well as chemical treatments both pre- and post-mechanical processes [4-6,34-36]. In the case of flax (*Linum usitatissimum*), the coarse bast fiber bundles that are isolated from the stem, termed technical fibers, are approximately 1 m in length and 50–100 μm in diameter. One technical fiber is made up of 10–40 individual fiber entities called elementary fibers, which are 2–5 cm in length and 10–20 μm in

diameter. Considering the tensile strength of elementary fibers of ~1300 MPa compared to that of technical fibers at ~600 MPa [10,34,36,37], a desired state of flax reinforcement is one where individual elementary fibers are well-dispersed (i.e. separated) and distributed (spread) within the polymer matrix.

There is a need for a robust processing technique that can compound natural fibers with a wide range of thermoplastic matrix options, and yield a composite morphology with highly debundled and distributed natural fibers, preferably at the level of elementary fibers. Solid-state shear pulverization (SSSP) is a developing technique for processing homopolymers, polymer blends, and polymer composites and nanocomposites that uses a modified TSE in a chilled, solid-state setting [38-46]. It applies shear and compression at temperatures well below T_m, T_g, and T_{deg} of the materials. While retaining the practical advantages of a TSE operation, the low-temperature nature of SSSP not only prevents undesirable thermal degradation, but also provides a pathway for composite development without limitations in viscosity, thermodynamics, and kinetics. The continuous, scalable process does not require monomers or solvents, and thus is environmentally benign. In sustainable materials research, SSSP has been applied to the processing of recycled plastics and bioderived polymers for two decades [38,39,43], and its use in biocomposites with lignocellulosic fillers have recently been reported [44-46]. The distinguished advantage of the SSSP process highlighted in prior polymer nanocomposites work is the ability to achieve prominent levels of filler exfoliation and dispersion in situ [40,41]. In applying the same principles to natural fibers, SSSP has the capability to debundle (fibrillate) and isolate the individual elementary fibers from technical fibers and simultaneously compound and distribute them in the polymer matrix in situ, without additional chemicals.

This paper presents the first study that applies the SSSP methodology to the compounding of natural fibers with polymers, with a specific intention of achieving consistent elementary fiber dispersion in high temperature-melting engineering thermoplastics. The study is conducted with a model system of flax and polyamide 6 (PA6); flax is one of the most practical natural fibers for composite applications today [9], and PA6 is a common engineering plastic often used in automotive, aerospace, and electronic applications. Due to the polymer processing temperatures above 250°C compared to the flax fiber T_{deg} of 200°C, conventional

melt compounding of PA6 with flax has been limited [47-49]. The viability of solid-state compounding of PA6/ flax is assessed via comparison of the composite morphology and physical properties with those from conventional TSE-compounding and hand-blending control. Furthermore, three different forms of flax fibers were compared for an insight into the optimal type of flax fibers with SSSP processing.

EXPERIMENTAL

Materials

The polymer matrix was a commercial extrusion grade PA6 resin, generously provided by BASF Corporation (Ludwigshafen, Germany), with a reported density of 1.13 g/cm^3 and MFI of 130 g/10 min (275^{o}C, 5.00 kg). Three types of flax fiber materials were used as the filler material. The first two types were processed short fibers from native Belgian flax, obtained from Algemeen Belgisch Vlasverbond (Kortrijk, Belgium). The flax stems had undergone a biological retting process in which waxes and pectin were removed, resulting in a material containing ~35 wt% fibers and ~65 wt% nonfiber shives [6]. This form of flax is the first fiber type, termed straw flax (st), cut nominally in 2-mm lengths. The flax material that had gone through a further scutching process [4-6] contains essentially pure fibers, and this form is the second type. These scutched fibers (sc) were also cut nominally in 2mm lengths. The third fiber type is a commercially available, refined flax sheet FlaxTape 200, obtained from S.A.S. Lineo (Saint-Martin-Du-Tilleul, France). FlaxTape (ft) was manually cut in 25 mm strips in the length-wise direction using a guillotine cutter.

Composite Processing

SSSP was conducted with a modified KrausMaffei Berstorff (Hanover, Germany) ZE-25A UTX co-rotational, intermeshing twin screw extruder (L/D=35, D=25 mm), in which the barrels are continuously cooled with a recirculating ethylene glycol/ water solution maintained at -12^{o}C by a Budzar BWA-AC10 industrial chiller. A custom compounding screw configuration, with eight bilobe kneading elements (5.8 L/D) spread over the screw length, was designed to effectively debundle flax fibers while minimizing

scission and overall physical damage to the fibers; two large forward-driving elements near the polymer inlet is designed for pellet size reduction, the subsequent two large forward plus one small neutral elements are designated for pulverizing the polymer, and the last three small forward elements are designed to compound the flax fibers with the polymer. The balance of the screw are constructed with conventional helical conveying elements. Figure 1 illustrates the screw configuration and barrel temperature profile of the SSSP compounding process. Compounding was conducted under atmospheric pressure, with a screw rotation speed of 200 rpm. The total throughput of 400 g/hr was provided from two inlets; PA6 pellets were fed upstream (2 L/D) with a Brabender Technologie RT-1.5 volumetric rototube feeder, while the flax fibers were metered into a down-stream port (27 L/D) with a Brabender Technologie DS28. The output was a continuous stream of flakes. A more detailed description of SSSP is available elsewhere [38, 39].

TSE compounding was conducted under vacuum in a Leistritz (Nürnberg, Germany) ZSE 18 MAXX co-rotational, inter-meshing twin-screw extruder (L/D =36, D=19 mm), with the barrel temperature set at 245°C. The screws were configured for conventional natural fiber compounding, with 11 bilobe kneading elements (4.5 L/D) and one mixing element (0.75 L/D), with the balance conventional helical conveying elements. The screw speed was set at 200 rpm. A total throughput of 3000 g/hr came from two ports, similarly to SSSP; PA6 pellets were fed with a weigh-in-loss feeder upstream (2 L/D), while the flax fibers were metered from a side screw half-way down the stream (18 L/D), both integrated within the Leistritz extruder system. A non-compounded, benchmark sample of the PA6/flax mixture was prepared by manually dry-blending the flax fibers with the PA6 material that had been pulverized by SSSP alone using the above conditions.

All of the PA6/flax samples were made with a consistent 20 wt% (as-received basis) flax fiber content. The PA6 pellets and flax fibers were the only materials processed; no compatibilizers or additives were used. Consistent drying, processing, and storing conditions were ensured for all the samples; polymer and flax were pre-dried in a convection oven at 80°C overnight prior to compounding, and all compounded samples were dried again for at least 1 day before injection molding. A DSM (Sittard, the Netherlands) Xplore micro-injection molder was used to prepare rectangular slabs and tensile test coupons according to

ASTM D790 and ASTM D638 standards, respectively. Injection molding was performed at a barrel temperature of 250°C and a mold temperature of 50°C, with the injection pressure set at 8 bar.

Sample Nomenclature

The samples are identified with a systematic nomenclature (e.g. "TSEsc") referring to the compounding method and the flax type used. The nomenclature NEAT is designated for the unfilled PA6 in the as-received pellet form, serving as the control sample. The MIX prefix refers to the manual dry-blending method, while TSE and SSSP are the two compounding methods studied. As for the suffix, st refers to straw flax (originally 2 mm fibers), while sc is scutched flax (2 mm fibers) and ft is FlaxTape (25 mm fiber strips).

Characterization

For 3-D composite morphology characterization with computer-aided micro-tomography (CT), a gauge section of an injection-molded tensile coupon was examined side-on in a General Electric (Wunstorf, Germany) Phoenix Nanotom, using a fast-scan mode with the voxel size of 2.5 μm. The X-ray from a molybdenum target operated at 60 kV and 174 μA. A scan volume of 5 mm x 1.5 mm x 5.75 mm was reconstructed into a 3-D image, which was analyzed in the Skyscan (Kontich, Belgium) CTVox and Data Viewer software. The flax fibers were isolated from the composite specimens via dissolution of PA6 in boiling phenol (Grade P9346, Sigma-Aldrich, St. Louis MO, USA) under reflux. The extracted, dried fibers were imaged on a silicon wafer using a Leica EZ4 HD stereomicroscope at the highest magnification. For fiber dispersion characterization, Injection-molded tensile coupon pieces were placed in an epoxy puck, and the plane perpendicular to the injection molding flow direction was sanded and polished. A Leica (Wetzlar, Germany) optical microscope with a Zeiss (Göttingen, Germany) Axiocam ERc5s camera was used to capture the cross section images of the fibers in a composite. Scanning electron microscopy (SEM) was used to examine the fiber-matrix interface upon applying load. The cross section of a tensile-fractured

coupon was sputter-coated with gold and examined in a Philips (Eindhoven, the Netherlands) XL30 field emission gun microscope in a secondary electron imaging mode, at an accelerating voltage of 5 kV and spot size of 3.

Mechanical property measurements, in both uniaxial tensile and three-point bending modes, were conducted on an Instron (Norwood, MA, USA) Model 4467 instrument with a 1 kN load cell. Tensile test, based on ASTM D638, employed flat pneumatic grips. Three-point bending, based on ASTM D790, used a fixture with 8 mm diameter rolls that were 40 mm apart at the base. All tests were conducted at room temperature, at a crosshead speed of 10 mm/min.

RESULTS AND DISCUSSION

Scutched Fiber Compounding

The initial discussion is the comparison of the three fiber incorporation methods (MIX, TSE, and SSSP) by focusing on the samples with scutched fibers (sc), which is the simplest but purest of the three fiber types. Figure 2 shows the photographs, taken in identical lighting conditions, of the three samples and the unfilled polymer control (NEAT), prior to injection molding at 250°C. The type of compounding clearly dictated its output form and color. The MIX sample is a manual blend of 80 wt% PA6 flakes (white) with 20 wt% scutched flax fibers (tan), without exposure to heat or compounding, and the appearance reflects those conditions. TSE output was in the form of brown pellets, typical of melt-compounded products of flax with other thermoplastics. The uniformity of color suggests good distribution of the flax fiber throughout the polymer matrix. However, the darker color suggests that melt-compounding in TSE led to thermal degradation of flax [29,30], and possibly of the PA6 [50], even though the materials were pre-dried and extrusion was conducted under vacuum with a relatively low temperature profile. SSSP compounding resulted in a flake output, with minimal visual sign of polymer or fiber degradation, especially in comparison with the TSE output. In addition, note that while MIXsc and SSSPsc are both of 20wt% fiber content and have similar flake appearance and particle sizes, SSSPsc sample appears to contain considerably more flax fibers in the image, simply based on the tan/white color contrast. This enhancement

in apparent fiber presence implies that the SSSP process caused separation of flax fibers into multiple diffused entities, which occupied a larger bulk volume of the resulting composite sample.

Upon subsequent injection molding, the color of the molded coupons from each respective sample was uniform, but considerably darker compared to before molding, as some thermal degradation of the materials could not be avoided at 250°C. Mieck et al. has reported that flax fibers show significant damage after an exposure time of 4 minutes at temperature above 240°C [51]. The molding process in this study using the benchtop equipment involved cycle times of approximately 3 minutes per injection. Practically, the composite samples would be less susceptible to thermal degradation considering that commercial scale injection molding can take less time, depending on the dimensions of the product and the injection-molding equipment used.

Composite Morphology Comparison

The 3-D filler morphology of in the injection-molded specimens was examined using micro CT, and the scan images are shown in Figure 3. A few common observations can be made for all three samples. First, the flax fiber entities are well-distributed throughout the tomography volume. Based on the uniform color distribution in the molded specimens discussed earlier, one can reasonably deduce that good filler distribution extends to the whole molded samples. Second, the flax fibers preferentially oriented along the flow of the molten polymer in the mold, as indicated in the arrow in the figure. Regardless of the shape and size, the fibers followed the flow pattern and filled the mold volume. Quantitative analysis of the micro CT scans are provided in Table 1; fiber fraction and void fraction values, converted via component densities, confirm 22–24 wt% fiber content. The voids in the composites samples are due partially to the pressure limitations of the injection molder. The compounded samples, namely TSEsc and SSSPsc, resulted in lower void fraction than simple MIXsc, which suggests that (1) some molecular weight reduction of the matrix polymer occurred, and consequently the lower melt viscosity facilitated the flow of the material into the mold; and/or (2) debundling and size reduction of the fibers and subsequent distribution in the matrix allowed for gases to escape more easily from the initial void formation. The voids were often found in the

centerline along the molded direction, though not discernible from Figure 3 with the contrast settings used. Lastly, as the scan volume of the micro CT study does not extend to the entirety of the molded specimens, Figure 3 images do not illustrate the potential skin-core effect, i.e. the difference in the fiber distribution at the outer edges of the molded specimens.

The more important, differentiating observation of Figure 3 is that the fiber width and lengths results are very different from each other. The MIXsc sample contains essentially the scutched flax fibers as-supplied, with lengths retained at ~2 mm. The diameters (thicknesses) of flax fibers are substantial, especially in contrast with other samples, indicating that the technical fibers remained bundled. TSE compounding, on the other hand, was able to debundle the fibers, as indicated by significantly smaller cross-fiber dimensions in Figure 3(b). However, the method was not able to keep the fiber lengths intact; the fibers were unnecessarily scissioned down to short fiber segments. Figure 3(c) shows that SSSP compounding resulted in appreciable debundling of technical fibers, in a similar fashion to TSE, while the fiber lengths were preserved remarkably well, on the order of millimeters.

For a further investigation of the debundling effects by the different compounding methods, the flax fibers were extracted from the composite specimens, and their macrostructure and dimensions were evaluated. Figure 4 clearly shows that as-received scutched flax fibers are in the form of technical fibers, whose diameters are on the order of 100 μm. Upon being hand-blended with PA6 and injection-molded, some ends of the technical fibers separate, while most technical fibers remain intact. Compounding prior to injection molding is necessary to debundle the technical fibers to elementary fibers. Figures 4(c) and (d) indicate that both TSE and SSSP are capable of separating individual elementary fibers, but a noticeable difference in the length-wise dimensions of the elementary fibers can be observed between TSE and SSSP. The TSE sample image contains fibers of 200–500 μm in length while that of SSSP shows fibers that are 500–1500 μm long. These representative fiber shapes and dimensions are confirmed by image analysis conducted in the 2-D projection from micro CT micrographs, though shorter and finer fibers are additionally observed in the CT micrographs.

Figure 5 presents the stereomicroscope images of the cross sections of the composites perpendicular to the injection mold flow direction. The images capturing the edge-on dimensions of the fibers confirm the fiber morphology trends in Figures 3 and 4; MIXsc sample contain still bundled technical fibers, whereas TSEsc, and SSSPsc to a lesser extent, has debundled and dispersed the individual elementary fibers.

General morphology conclusions can be drawn from the micro CT and optical microscope observations. The undeveloped morphology in MIXsc sample is expected, as the sample did not undergo any compounding, and injection molding flow is not sufficient to separate bundled technical fibers or affect the lengths of the fibers. Compounding the scutched fibers with PA6, either in the melt or the solid state, led to effective debundling and yielded elementary fibers. However, the significant reduction in fiber lengths observed in TSE sample, in Figures 3(b) and 4(c), suggests that shortening of the fibers were caused by the thermal degradation of the fibers discussed earlier [29, 30]. Considering that TSE and SSSP compounding were conducted with similarly moderate screw configurations and under similarly short residence time, the onset of thermal degradation is speculated to cause a nearly immediate and drastic deterioration of tensile strength and ductility in flax elementary fibers. Therefore, SSSP compounding is capable of providing shearing forces to separate the elementary fibers while the low-temperature operation retains the lengths of the fibers intact.

Mechanical Properties of the Composites

The mechanical performance of the composites is expected to reflect the differences in the morphology observed above. Tensile and three-point bending test results of NEAT and the three PA6/ 20 wt% scutched flax composites are presented in Figure 6. In terms of stiffness, the addition of scutched flax enhanced both tensile and flexural moduli of PA6 significantly. The modulus increase is expected because the reported elastic modulus of flax is 45–60 GPa [10,34,36,37]. However, the extent of stiffness enhancement is dictated by the processing methodology. The SSSP-compounded composite exhibited 3.2 and 2.4 times the tensile and flexural moduli, respectively, compared to the unfilled base PA6 material, and these improvement levels are significantly higher than those observed in the MIX and the TSE-compounded

composites; to the authors' knowledge, these stiffness enhancement values in the SSSP sample are the highest reported for compounded PA6/ 20wt% flax in the literature.

As for tensile and flexural strengths, on the other hand, incorporation of flax into PA6 resulted in a non-appreciable increase across the three different methods, in spite of the tensile strength of even the technical fibers being an order of magnitude higher than that of neat PA6. Figure 6 suggests a tendency that SSSP compounding has the most positive effect in enhancing the strengths of PA6; SSSPsc has a modest 20% increase in tensile strength compared to NEAT. However, the rest of the tensile strengths and all of flexural strengths exhibit values that are statistically invariant compared to those of NEAT. The hand-mixed PA6/scutched flax fiber composite even shows a decrease in flexural strength. Lastly, in terms of ductility, the strain at break of the polymer is significantly compromised via the incorporation of flax; this is expected from the general composite principle; the reported breaking strain of flax is 2 % [34,36].

Before discussing the structural causes of the observed properties, it is worth commenting on the differences in mechanical property values obtained from tensile vs. 3-point bending tests, where the latter set is always higher. Several possible explanations exist for this phenomenon. First, the flexural modulus and strength are calculated from the classical beam theory [52], which assumes that the stress-strain profile from the neutral axis to the outer edges of the beam are triangular, while in reality this shape is nonlinear, which results in overestimated flexural values [53]. Second, whereas the stresses in a tensile test are uniform throughout the specimen cross-section, the stresses under bending vary from zero in the middle to a maximum at the top and bottom surfaces in the center of the sample [52]. Because the injection molding process tends to align the fiber in the outer regions of the molded specimens parallel to the mold fill direction, according to the skin-core effect [54], more highly-oriented fibers concentrate in the area where maximal flexural stresses are measured, and thus flexural moduli and strengths are most likely overestimated. Third, based on the same non-uniform stress measurements in bending mode argument, flexural tests are less sensitive to the macro defects (e.g. voids) present in the center of the molded samples. Given the earlier discussion that injection molding process led to some void formation (Table 1) in the

center of the specimens, tensile results reflected these center defects more prominently via dramatic reductions in stiffness and strength.

Composite Morphology-Property Relations

To understand the relationship between the observed mechanical behaviors and the composite morphology features caused by differing flax compounding methods, appropriate composite models based on rules of mixtures, were employed to qualitatively compare the morphological features as well as determine overall efficiencies of the samples.

For an elastic modulus of a short fiber composite (E_c), the Cox-Krenchel model, Eq. 1, takes into account the effects from fiber lengths and fiber orientation [56,57].

$$E_c = \eta_{O,E}\,\eta_{L,E}\,\nu_f\,E_f + (1-\nu_f)E_m \quad (1)$$

The variables E_f and E_m are the fiber and matrix elastic moduli, ν_f is the fiber volume fraction, $\eta_{O.E}$ is the fiber orientation factor, and $\eta_{L,E}$ is the fiber length efficiency factor. Eq. 2 defines $\eta_{O.E}$ as follows [57]:

$$\eta_{O,E} = \sum_n a_n \cos^4 \phi_n \quad (2)$$

where a_n and ϕ_n are the fraction and orientation angle, respectively, of the nth fiber in the morphology. The example values of $\eta_{O.E}$ are 0.375 for in-plane random distribution, and 0.2 for 3-D random distribution. Length efficiency factor is determined from Eq. 3.

$$\eta_{L,E} = 1 - \frac{\tanh\left(\frac{\beta L}{2}\right)}{\left(\frac{\beta L}{2}\right)} \quad (3)$$

The quantity L is the fiber length and β is defined by Eq. 4, for a square geometrical packing case [58].

$$\beta = \frac{2}{d}\left(\frac{2\,G_m}{E_f \ln\sqrt{\pi/4\nu_f}}\right)^{\frac{1}{2}} \quad (4)$$

In Eq. 4, d is the fiber diameter and G_m the shear modulus of the matrix. The polymer matrix is assumed to be isotropic, and thus G_m relates to the material E_m and Poisson's ratio, υ, according to Eq. 5.

$$G_m = \frac{E_m}{2(1+\upsilon)} \quad (5)$$

The lowest modulus value measured in this study came from the TSEsc specimen (Figure 6(a)). The melt compounding methodology managed to isolate elementary fibers but was thermally too harsh to keep the fiber lengths, which results in low $\eta_{L,E}$ value as well as reduced $\eta_{O.E}$ in Eq. 1. On the other hand, Figures 3 and 4 suggest that the MIXsc and SSSPsc samples contain longer fibers on the order of millimeters, and therefore their higher stiffness values reported in Figure 6(a) had contributions from high length efficiencies. Between the two, however, the MIXsc did not have as high of a modulus enhancement as SSSPsc. Earlier, Figure 5 revealed that the lack of compounding kept the flax fibers in MIXsc mostly in their original, bundled technical fibers state. Based on previous studies that have reported slightly lower tensile modulus for technical fibers (~45 GPa) in reference to elementary fibers (60 GPa) [10,34,36,37], the E_f quantity in Eq. 1 is then an averaged technical/elementary fiber stiffness, which would be lower for MIXsc than SSSPsc. Further, the significantly higher void content reported in Table 1 for MIXsc suggests that adhesion between the fibers and the polymer matrix may not have been as effective as the SSSPsc sample, which would contribute to a lower modulus.

As a comparison to the highest tensile modulus reported in this study, 5.5 GPa for SSSPsc, the maximum attainable modulus for a theoretical PA6/flax composite is calculated to be 10.6 GPa via Equations 1–5, using orientation factor $\eta_0 = 1$; $E_f = 60$ GPa [10,36]; $E_m = 1.68$ GPa (measured, Figure 6(a)); $L = 2$ mm (nominal fiber length); $v_f = 0.16$ (measured in SSSPsc, Table 1); $d = 15$ µm [34]; $\upsilon = 0.4$ (reported by the manufacturer). Alternatively, the combined effective efficiency, as defined as $\eta = \eta_{O.E}\,\eta_{L,E}$ in Eq. 1, was calculated to be 0.43 for the same sample.

The strength enhancement of PA6 with flax is overall modest compared to the changes observed in stiffness. Thomason and Vlug argue that an increase in short fiber composite strength will be noticeable when the fiber aspect ratio is greater than 50 [58]. In MIXsc, even though the lengths are retained up to 2 mm (Figures 3(a) and 4(b)), the technical fiber diameters on the order of 100 µm (Figure 5(a)) lead to apparent aspect ratios near 20, which are not sufficient for a significant strength improvement. Indeed, a necessary requirement to improve the strength of PA6/flax composites, with short 2 mm fibers, is to

effectively debundle flax into thinner and stronger individual elementary fibers. Even though both TSE and SSSP compounding achieved elementary fibers, the unnecessary shortening of the fibers in TSEsc have aspect ratios below 50, while those in SSSPsc are reaching above 50.

As an analogy to the Cox-Krenchel model, Kelly-Tyson model is used to evaluate the composite strength (σ_c), as given in Eq. 6 [59].

$$\sigma_C = \eta_{0,S}\,\eta_{L,S}\,\nu_f\,\sigma_f + (1-\nu_f)\sigma_m \quad (6)$$

In the Kelly-Tyson model, $\eta_{O,S}$ is the identical fiber orientation factor to $\eta_{O,E}$ in Equation 2, $\eta_{L,S}$ is the fiber length efficiency as defined in Equation 7, σ_f is the fiber tensile strength, and σ_m is the matrix tensile strength.

$$\eta_L = \frac{1}{\nu_f}\left[\sum_{subcritical}\frac{L_i}{2L_c}\nu_{f,i} + \sum_{supercritical}\left(1-\frac{L_c}{2L_j}\right)\nu_{f,j}\right] \quad (7)$$

where $\nu_{f,i}$ is the volume fraction of fibers with lengths L_i below the critical length (L_c), $\nu_{f,j}$ is the volume fraction of fibers with lengths L_j above L_c. The value of L_c is determined as follows:

$$L_c = \frac{\sigma_f d}{2\tau} \quad (8)$$

where τ is the intrinsic interfacial shear strength (IFSS) of the fiber-matrix pair, and d is the fiber diameter.

Qualitative comparisons of the observed fiber lengths in the composite samples to the critical fiber length is a good way to evaluate the effectiveness of strength enhancements; if a fiber in the composite is shorter than the critical fiber length, it would not be loaded up to their failure stress within the compound. Adopting the IFSS of flax/polyamides as 22 MPa from a prior work by Le Duigou et al. [60], L_c of technical fibers (d = 75 µm) is calculated to be 1700 µm, while L_c of elementary fibers (d = 15 µm) is 1000 µm. Figures 3 and 4 indicate that MIXsc sample contains technical fibers, most of which have the length below this technical fiber L_c. Similarly, TSEsc has elementary fibers, most of which are significantly shorter than the elementary L_c. On the contrary, the SSSP-compounding technique was able to produce a composite with higher strength compared to NEAT, because the length of the debundled fibers lie above the elementary L_c, and additionally the occasional bundled technical fibers remain long near or above the technical L_c. This

implies that both the elementary and technical fibers of the SSSPsc sample can be loaded up to their failure stress in the composite.

Similarly to the modulus analysis above, the maximum attainable strength can be calculated with theoretical parameter values. These involve $\eta_0 = 1$; $\sigma_f = 1300$ MPa [10,34,36]; $\sigma_m = 64$ MPa (measured, Figure 6(b)); $L_c = 1000$ μm; $v_{f,i} = 0$; and $v_{f,j} = 1$. With these values, the maximum attainable strength is 216 MPa, compared to the highest tested tensile strength, for SSSPsc, of 88 MPa. Alternatively, the combined effective strength efficiency, as defined as $\eta = \eta_{O,S}\,\eta_{L,S}$ in Eq. 6, was calculated to be 0.16 for the SSSPsc sample.

Keeping in mind that, for both modulus and strength scenarios, an effective efficiency factor approaching 1 is essentially unrealistic, the modulus efficiency of 0.43 that was achieved via SSSP processing is reasonably high for a composite made from pure forms of flax and PA6 without any chemical modifications or compatibilizers. On the other hand, the strength efficiency of 0.14 has greater room for improvement. Figure 7 is the SEM micrograph of a tensile-fractured surface of an SSSPsc specimen; flax fibers, especially the bundled technical fibers, experience pull-out, rather than clean fiber break at the fractured surface, which suggests a sub-optimal fiber/matrix adhesion. This could the reason why the strength enhancement in SSSPsc is relatively small. Further investigation on the interface characteristics, including the IFSS determination for flax/PA6, as well as methods to enhance flax/polymer adhesion [2-4] during SSSP-compounding, is necessary, and currently underway. Once an optimized flax/PA6 composite system is established, quantitative composite models that account for the detailed morphology features of the flax fiber and polymer [61] can be subsequently pursued.

Effects of Flax Type

The final part of the study concerns different flax fiber types; straw flax and FlaxTape were processed with PA6 at the same fiber content and under identical SSSP compounding and injection molding conditions as the original scutched flax. Comparative 3-D composite morphology and fiber cross-section micrographs are provided in Figures 8 and 9, respectively. The SSSPst sample contains many fibers that

preserved the original lengths as well as thickness; Figure 9(b) reveals a co-existence of debundled elementary fibers and bundled technical fibers. On the other hand, Figures 8 and 9 show that the SSSPft has numerous, mostly isolated elementary fibers with shorter lengths around 500 μm, while SSSPsc contained both technical and elementary fibers with preserved lengths up to 1 mm. This is an important observation, as FlaxTape started with fibers more than 12-fold longer than scutched flax. Original length of the fiber material did not prove to be an important factor in SSSP-compounding with a polymer. A similar observation has been observed by Ausias and coworkers [55] for melt processing of flax. The unnecessary shortening of FlaxTape during SSSP may have its roots in its preparation steps. Compared to the base scutched flax, which is simply retted, scutched and chopped, FlaxTape undergoes additional steps of aligning and preserving the length of flax in a sheet form. The mechanical and chemical refinements required during these steps possibly had damaged the flax fibers, which perhaps became more susceptible to disintegration when subjected to external shearing and grinding by the SSSP process.

Mechanical property measurement results are summarized as bar charts in Figure 10, with line markers indicating the control NEAT and equivalent TSE-compounded sample properties. It is clear that the straw flax is not as effective at enhancing the mechanical properties of PA6 as other, more refined forms of flax fibers; in fact, the addition of straw flax to PA6 had a negative effect on the tensile and flexural strengths. Even though Table 1 shows that SSSPst measured a 26 vol% fiber content, only 35 vol% of the straw flax is fibrous and the other 65 vol% are shives [6]. This means that the actual fiber content of SSSPst was less than 10 vol%, and the other non-fibrous materials occupying the filler space may not have contributed as effectively to the modulus or strength enhancement. As there are often challenges with feeding short fiber particles into compounding extruders at high ratios, straw flax presents a practical limit to its potential in enhancing mechanical properties of polymers.

Comparing between the original 2 mm-scutched flax and refined FlaxTape, some of the tested mechanical properties are within experimental error and the FlaxTape sample is marginally superior to the scutched flax sample in tensile strength. Qualitative inspection of Figures 8(c) and 9(c) suggests that the aspect ratio of the SSSPft is around 50, which corresponds to the starting point of noticeable strength

improvements [58]. Based on the Kelly-Tyson critical length argument, SSSPft contains more elementary fibers with lengths above the L_c. In contrast, SSSPsc has less elementary fibers above L_c, though it also has a small portion of technical fibers that are above its L_c contributing to the composite strength. In the end, in SSSP compounding, the refined scutched flax is a sensible upgrade from the pure straw flax for better mechanical performance, but from a practicality and economic standpoints, the flax material does not need to be further refined beyond the industrial scutching step. Ensuring higher fiber content in the composite via effective and efficient flax fiber feeding and metering continues to be a key objective in continuous compounding methods like TSE and SSSP.

CONCLUSIONS

This work pushed the practical boundary of natural fibers' applicability in composite materials by showcasing that they can be effectively processed with polymer matrices whose conventional processing temperatures are considered too high for their thermal stability. Based on a model PA6/scutched flax composite, SSSP process exhibited a noteworthy improvement in stiffness and a moderate improvement strength compared to hand-mixed and TSE-compounded analogues, by way of debundling and dispersing of strong elementary fibers and retaining the fiber lengths. The investigation of the effect of the flax fiber type determined that the crude straw flax option yields composites with significantly lower moduli and strengths than those made with refined flax due to its shive content, while the length advantage of FlaxTape did not translate effectively to the composite property enhancement via SSSP compounding.

As engineering thermoplastic-based composite materials become increasingly prominent in industrial products made via processes like extrusion, thermoforming, and injection molding, more systematic process-structure-property relation studies in biocomposite alternatives involving natural fibers and high temperature melting thermoplastics are warranted. Specifically, detailed fiber morphology characterization and quantitative composite model comparison studies with varying fiber content, interface compatibilization strategies, and SSSP compounding conditions are needed to fully understand the ability of natural fibers to enhance thermoplastics tailored to desired applications. After all, one effective way to

address today's sustainability challenges is to expand the design and use space of existing materials via innovative processing.

ACKNOWLEDGMENTS

Material support came from Dr. Ruth Lohwasser (BASF Performance Polymers) and Jan Demeulenaere (Algemeen Belgisch Vlasverbond). The SSSP equipment was funded by the NSF Major Research Instrumentation Grant (CMMI-0820993), and is under continued technical support from KraussMaffei Berstorff Corporation. The authors are indebted to many researchers at KU Leuven for their help with instruments and technical discussion: Dr. Oksana Shishkina and Delphine Depuydt (MTM/CMG), Karen Soete and Wim Six (Bruges/CMG), and Dr. Lien Telen (Chemistry). KW is grateful for the support from Belgian American Education Foundation Fellowship and Bucknell University Engineering Deans Fellowship.

REFERENCES

1. K.K. Chawla, *Composite Materials: Science and Engineering*, Springer (2012).
2. P.K. Mallick, *Fiber-Reinforced Composites: Materials, Manufacturing, and Design*, Marcel Dekker (1993).
3. A.K. Bledzki and J. Gassan, *Prog. Polym. Sci.*, **24**, 221 (1999).
4. A.K. Mohanty, M. Misra, and L.T. Drzal, Eds., *Natural Fibers, Biopolymers, and Bio-Composites*, CRC Press (2005).
5. S. Kalia, B.S. Kaith, and I. Kaur, Eds., *Cellulose Fibers: Bio- and Nano-Polymer Composites*, Springer (2011).
6. R.R. Franck, Ed., *Bast and Other Plant Fibres*, Elsevier (2005).
7. P. Wambua, J. Ivens, and I. Verpoest, *Compos. Sci. Tech.*, **63**, 1259, (2003).
8. L.A. Burglund and T. Peijs, *MRS Bull.*, **35**, 201 (2010).
9. L. Pil, F. Bensadoun, J. Pariset, and I. Verpoest, *Composites Part A*, **83**, 193 (2016).
10. A. Bourmaud, J. Beaugrand, D.U. Shah, V. Placet, and C. Baley, *Prog. Mater. Sci.*, **97**, 347 (2018).
11. J. Holbery and D. Houston, *JOM*, **11**, 80 (2006).
12. E. Bodros, I. Pillin, N. Montrelay, and C. Baley, *Compos. Sci. Tech.*, **67**, 462 (2007).
13. G. Koronis, A. Silva, and M. Fontul, *Composites Part B*, **44**, 120 (2013).
14. V.K. Thakur, M.K. Thakur, P. Raghavan, and M.R. Kessler, *ACS Sustainable Chem. Eng.*, **2**, 1072 (2014).
15. K. Stade, *Polym. Eng. Sci.*, **17**, 50 (1977).
16. K. Eise, J. Curry, and J. Farrell, *Polym. Eng. Sci.*, **25**, 497 (1985).
17. T. Villmow, B. Kretzschmar, and P. Potschke, *Compos. Sci. Tech.*, **70**, 2045 (2010).
18. M.S. Salit, M. Jawaid, N.B. Yusoff, and M.E. Hoque, Eds., *Manufacturing of Natural Fiber Reinforced Polymer Composite*, Springer (2015).
19. N. Barkoula, S. Garkhail, and T. Peijs, *J. Reinf. Plast. Compos.*, **29**, 1366 (2010).
20. H.L. Bos, J. Müssig, and M.J. van den Oever, *Composites Part A*, **37**, 1591 (2006).
21. G. Cantero, A. Arbelaiz, R. Llano-Ponte, and I. Mondragon, *Compos. Sci. Tech.*, **63**, 1247 (2003).
22. K.L. Pickering, G.W. Beckermann, S.N. Alam, and N.J. Foreman, *Composites Part A*, **38**, 461 (2007).
23. K. Jayaraman, *Compos. Sci. Tech.*, **63**, 367 (2003).

24. X. Li, L.G. Tabil, I.N. Oguocha, and S. Panigrahi, *Compos. Sci. Tech.*, **68**, 1753 (2008).

25. J.R. Araujo, W.R. Waldman, and M.A. De Paoli, *Composites Part A*, **37**, 1591 (2006).

26. F. Yao, Q.L. Wu, Y. Lei, and Y.J. Xu, *Ind. Crops Prod.*, **28**, 63 (2008).

27. K. Oksman, M. Skrifvars, and J.F. Selin, *Compos. Sci. Tech.*, **63**, 1317 (2003).

28. C. Nyambo, A.K. Mohanty, and M. Misra, *Biomacromolecules*, **11**, 1654 (2010).

29. J. Gassan and A. Bledzki, *J. Appl. Polym. Sci.*, **82**, 1417 (2001).

30. F. Yao, Q.L. Wu, Y. Lei, W.H. Guo, and Y.J. Xu, *Polym. Degrad. Stab.*, **93**, 90 (2008).

31. C.A.S. Hill, A. Norton, and G. Newman, *J. Appl. Polym. Sci.*, **112**, 1524 (2009).

32. A. Bismarck, I. Aranberri-Askargorta, J. Springer, T. Lampke, B. Wielage, A. Stamboulis, I. Shenderovich, and H.-H. Limbach, *Polym. Compos.*, **23**, 872 (2002).

33. K. Van de Velde and P. Kiekens, *Polym. Test.*, **20**, 885 (2001).

34. H.L. Bos, M.J.A. van den Oever, and O.C.J.J.Peters, *J. Mater. Sci.*, **37**, 1683 (2002).

35. T. Zimmermann, E. Pöhler, and T. Geiger, *Adv. Eng. Mater.*, **6**, 754 (2004).

36. C. Baley, *Composites Part A,* **33**, 939 (2000).

37. D. Depuydt, K. Hendrickx, W. Biesmans, J. Ivens, and A.W. Van Vuure, *Composites Part A*, **99**, 76 (2017).

38. N. Furgiuele, A.H. Lebovitz, K. Khait, and J.M. Torkelson, *Macromolecules*, **33**, 225 (2000).

39. K. Khait, S.H. Carr, and M.H. Mack, *Solid-State Shear Pulverization: A New Polymer Processing and Powder Technology*, Technomic (2001).

40. A.M. Walker, Y. Tao, and J.M. Torkelson, *Polymer*, **48**, 1066 (2007).

41. K. Wakabayashi, C. Pierre, D.A. Dikin, R.S. Ruoff, T. Ramanathan, C.L. Brinson, and J.M. Torkelson, *Macromolecules*, **41**, 1905 (2007).

42. J. Masuda and J.M. Torkelson, *Macromolecules*, **41**, 5974 (2008).

43. E.V. Miu, A.J. Fox, S.H. Jubb, and K. Wakabayashi, *J. Appl. Polym. Sci.*, **133**, 43070 (2016).

44. K.A. Iyer and J.M. Torkelson, *Polym. Compos.*, **34**, 1211 (2013).

45. K.A. Iyer, G.T. Schueneman, and J.M. Torkelson, *Polymer*, **56**, 464 (2014).

46. K.A. Iyer and J.M. Torkelson, *ACS Sustain. Chem. Eng.*, **3**, 959 (2015).

47. E. Ozen, A. Kiziltas, E.E. Kiziltas, and D.J. Gardner, *Polym. Compos.*, **34**, 544 (2013).

48. A. Elsabbagh, L. Steuernagel, and J. Ring, *Composites Part B*, **108**, 325 (2017).

49. F.C. Fernandes, R. Gadioli, E. Yassitepe, and M.A. De Paoli, *Polym. Compos.*, **38**, 299 (2017).

50. S.V. Levchik, E.D. Weil, and M. Lewin, *Polym. Int.*, **48**, 532 (1999).

51. K.-P. Mieck, A. Nechwatal, and C. Knobelsdorf, *Melliand Textilber.*, **11**, 892 (1994).

52. R.M. Jones, *Mechanics of Composites Materials*, CRC Press (1998).

53. W. Weibull, *J. Appl. Mech.,* **18**, 293 (1951).

54. S.F. Xavier, D. Tyagi, and A. Misra, *Polym. Compos.*, **3**, 88 (1982).

55. G. Ausias, A. Bourmaud, G. Coroller, and C. Baley, *Polym. Degrad. Stab.*, **98**, 1216 (2013).

56. H. L. Cox, *B. J. Appl. Phys.*, **372**, 72 (1952).

57. H. Krenchel, *Fibre Reinforcement: Theoretical and Practical Investigations of the Elasticity and Strength of Fibre-reinforced Materials*, Akademisk Forlag (1964).

58. J.L. Thomason and M.A. Vlug, *Composites Part A*, **27**, 477 (1996).

59. A. Kelly and W.R. Tyson, *J. Mech. Phys. Solids,* **13**, 329 (1965).

60. A. Le Duigou, A. Bourmaud, C. Gourier and C. Baley, *Composites Part A,* **85**, 123 (2016).

61. E. Lafranche, V.M. Oliveira, C.I. Martins, and P. Krawczak, *J. Compos. Mater.*, **49**, 113 (2015).

FIGURE CAPTIONS

FIG. 1. Screw configuration and barrel temperature profile of the SSSP set-up. The three types of bilobe kneading elements used in the screw configuration are pictured.

FIG. 2. (a) PA6 pellets (NEAT); and PA6/ 20wt% scutched flax samples via (b) hand blending (MIXsc), (c) melt-compounding (TSEsc), and (d) solid-state compounding (SSSPsc).

FIG. 3. Computer tomographs of injection-molded tensile test coupon sections of (a) MIXsc, (b) TSEsc and (c) SSSPsc specimens.

FIG. 4. Optical microscope images of scutched flax fibers from (a) as-received, prior to injection molding, and as isolated from injection-molded specimens of (b) MIXsc, (c) TSEsc and (d) SSSPsc.

FIG. 5. Optical microscope images of polished surface of (a) MIXsc, (b) TSEsc and (c) SSSPsc specimens. Left arrow points at an intact technical fiber bundle. Right arrow points at an individual elementary fiber.

FIG. 6. Effect of compounding techniques on (a) moduli and (b) strengths of PA6/ 20 wt% scutched flax fiber composites, in tensile (solid) and flexural (stripes) modes. Error bars represent ± one standard deviation.

FIG. 7. SEM image of the cross section of a failed SSSPsc tensile coupon.

FIG. 8. Computer tomographs of injection-molded tensile test coupon sections (a) SSSPsc, (b) SSSPst and (c) SSSPft specimens.

FIG. 9. Optical microscope images of polished surface of (a) SSSPsc, (b) SSSPst and (c) SSSPft specimens.

FIG. 10. Effect of flax type on (a) moduli and (b) strengths of PA6/ 20 wt% flax fiber composites, in tensile (solid) and flexural (stripes) modes. N and T benchmarks represent corresponding NEAT and TSE moduli and strengths, respectively. Error bars represent ± one standard deviation.

TABLE 1. Composite Samples: Morphology Analysis Summary

Sample ID	Measured Fiber Dontent (vol%)	Measured Void Content (vol%)	Calculated Fiber Content by Weight (wt%)
NEAT	--	--	--
MIXsc	17	0.9	24
TSEsc	15	0.2	22
SSSPsc	16	0.2	23

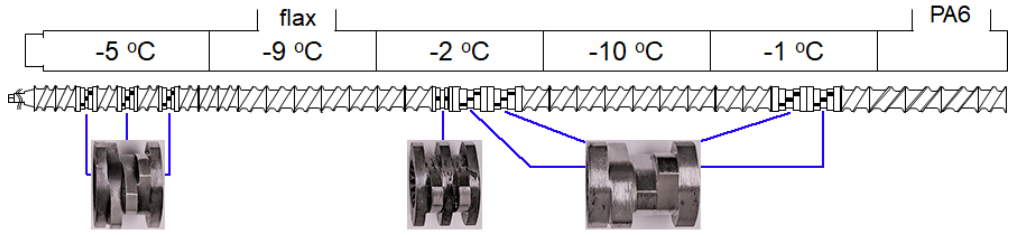

FIG. 1. Screw configuration and barrel temperature profile of the SSSP set-up. The three types of bilobe kneading elements used in the screw configuration are pictured.

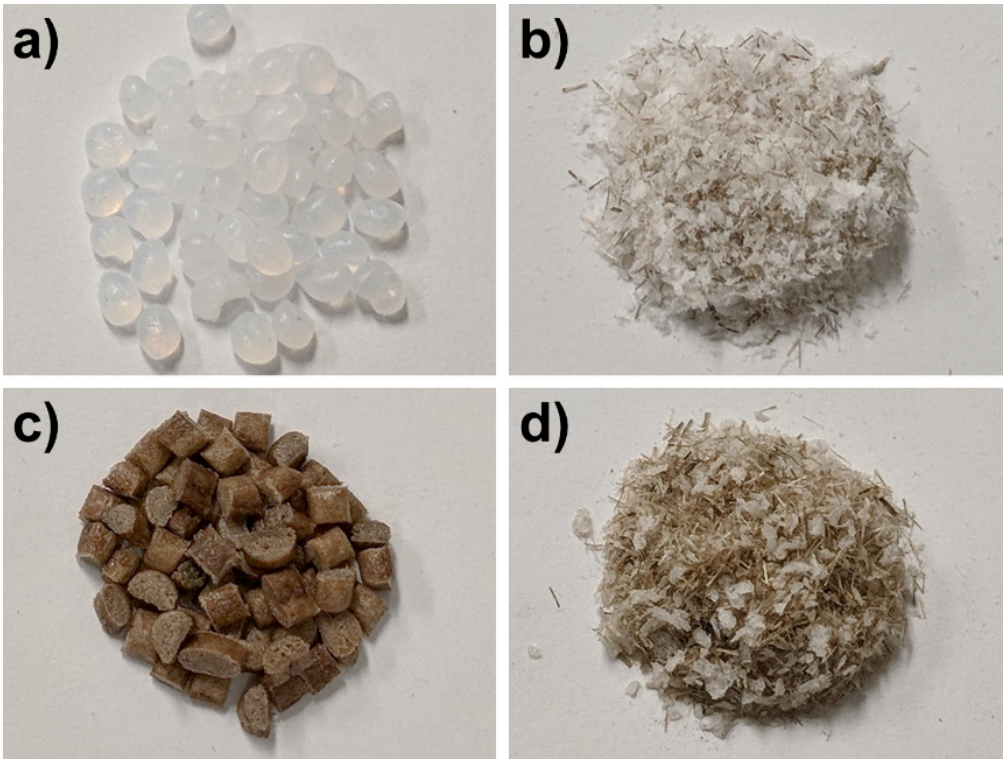

FIG. 2. (a) PA6 pellets (NEAT); and PA6/ 20wt% scutched flax samples via (b) hand blending (MIXsc), (c) melt-compounding (TSEsc), and (d) solid-state compounding (SSSPsc).

99x75mm (219 x 219 DPI)

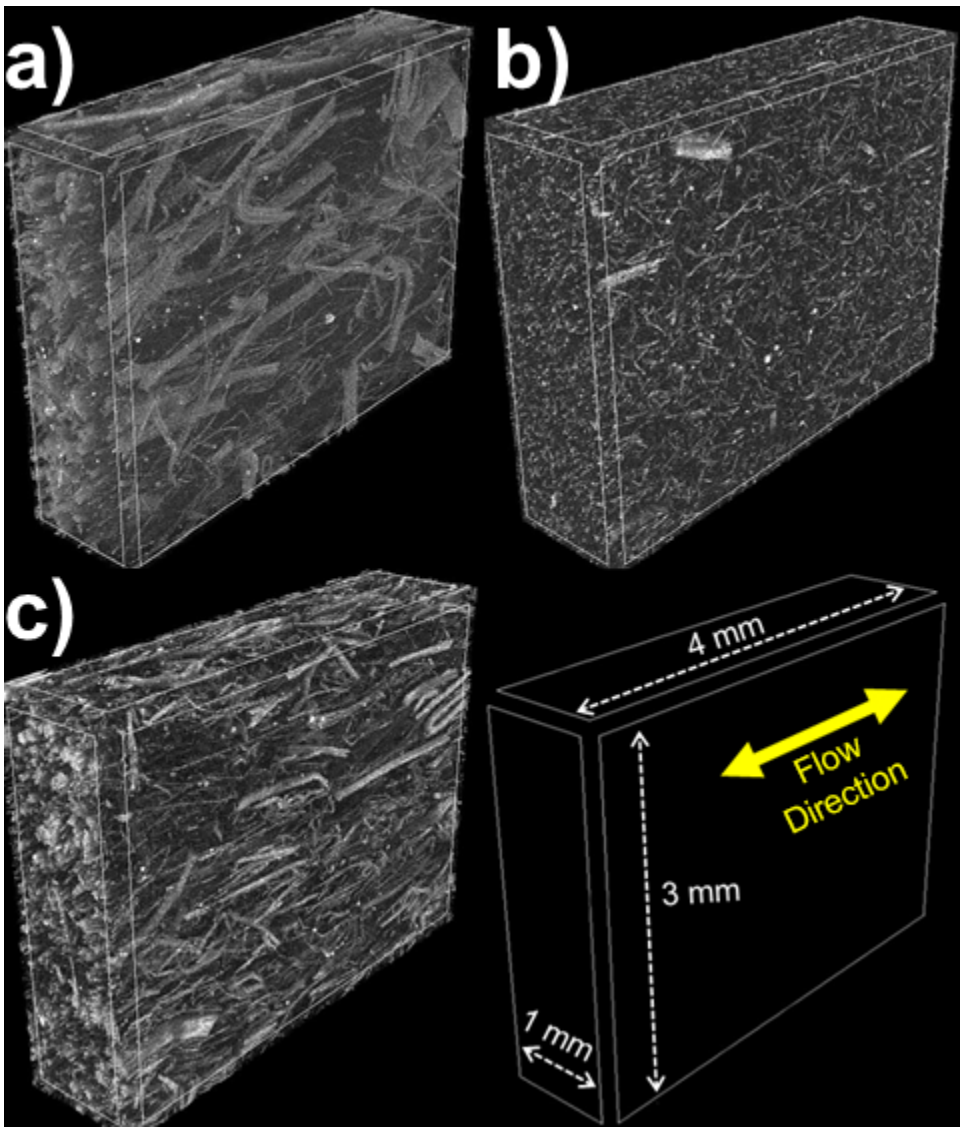

FIG. 3. Computer tomographs of injection-molded tensile test coupon sections of (a) MIXsc, (b) TSEsc and (c) SSSPsc specimens.

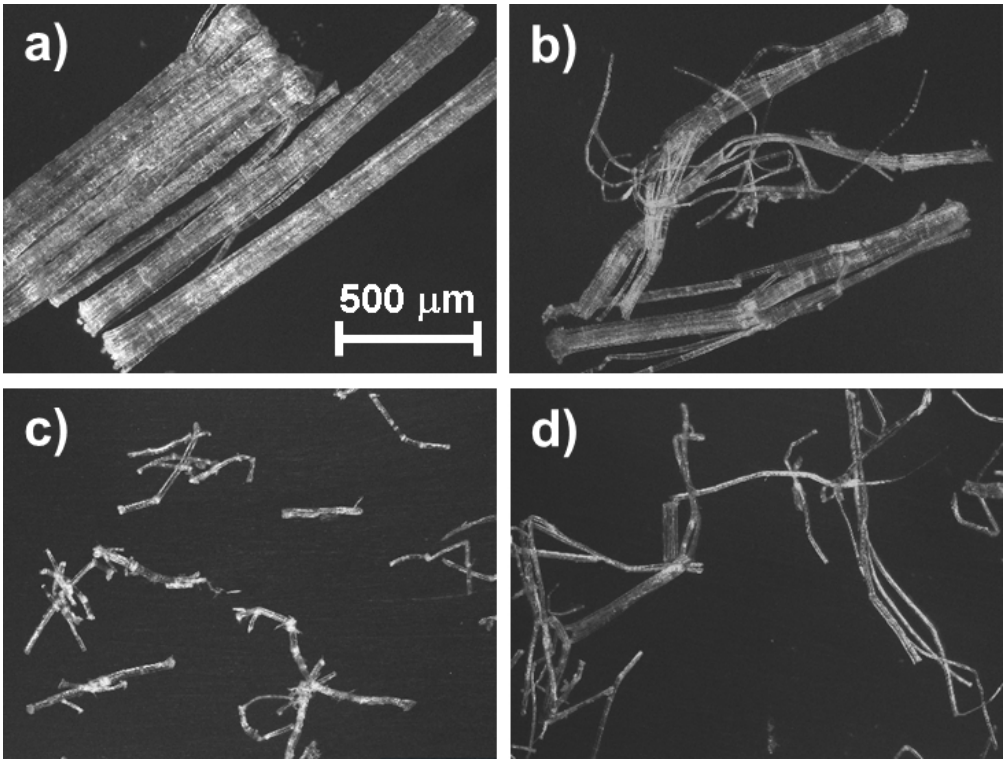

FIG. 4. Optical microscope images of scutched flax fibers from (a) as-received, prior to injection molding, and as isolated from injection-molded specimens of (b) MIXsc, (c) TSEsc and (d) SSSPsc.

124x93mm (149 x 149 DPI)

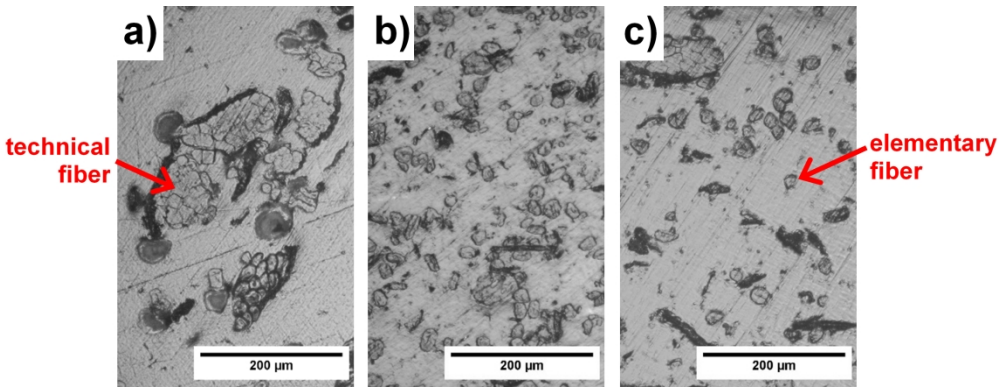

FIG. 5. Optical microscope images of polished surface of (a) MIXsc, (b) TSEsc and (c) SSSPsc specimens. Left arrow points at an intact technical fiber bundle. Right arrow points at an individual elementary fiber.

1001x381mm (96 x 96 DPI)

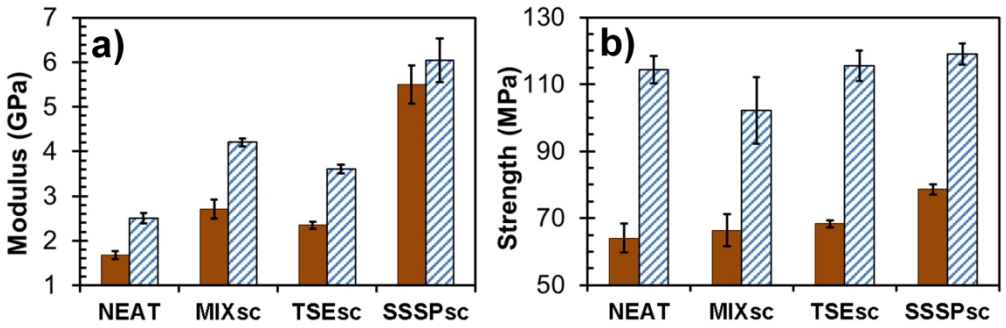

FIG. 6. Effect of compounding techniques on (a) moduli and (b) strengths of PA6/ 20 wt% scutched flax fiber composites, in tensile (solid) and flexural (stripes) modes. Error bars represent ± one standard deviation.

1022x327mm (96 x 96 DPI)

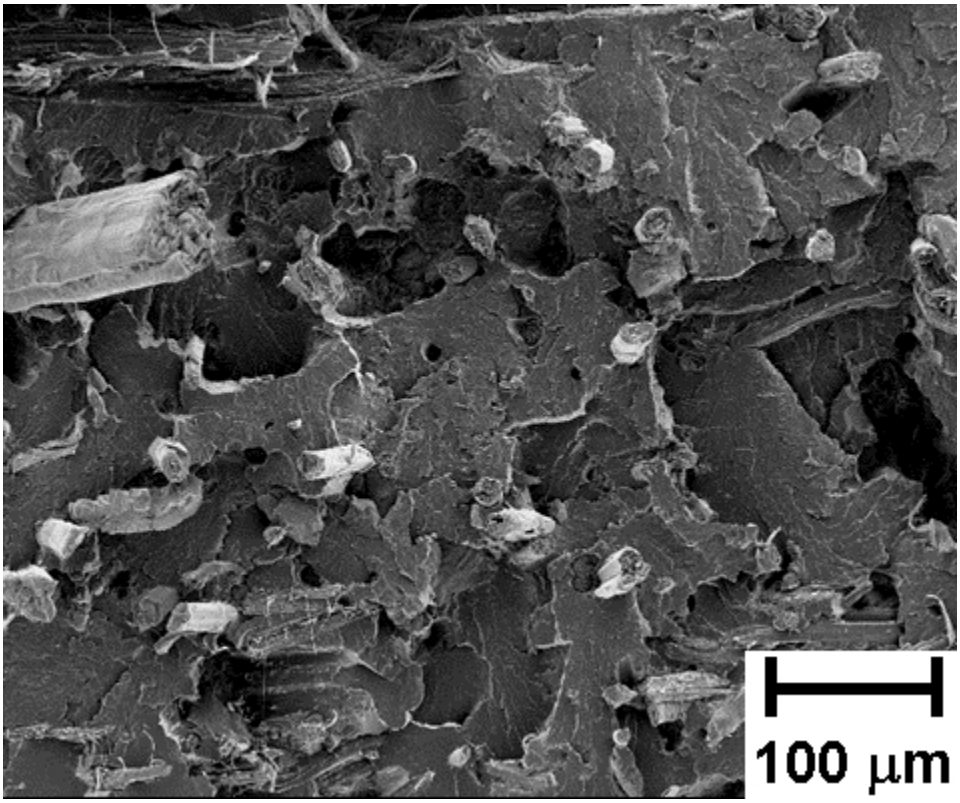

FIG. 7. SEM image of the cross section of a failed SSSPsc tensile coupon.

81x67mm (149 x 149 DPI)

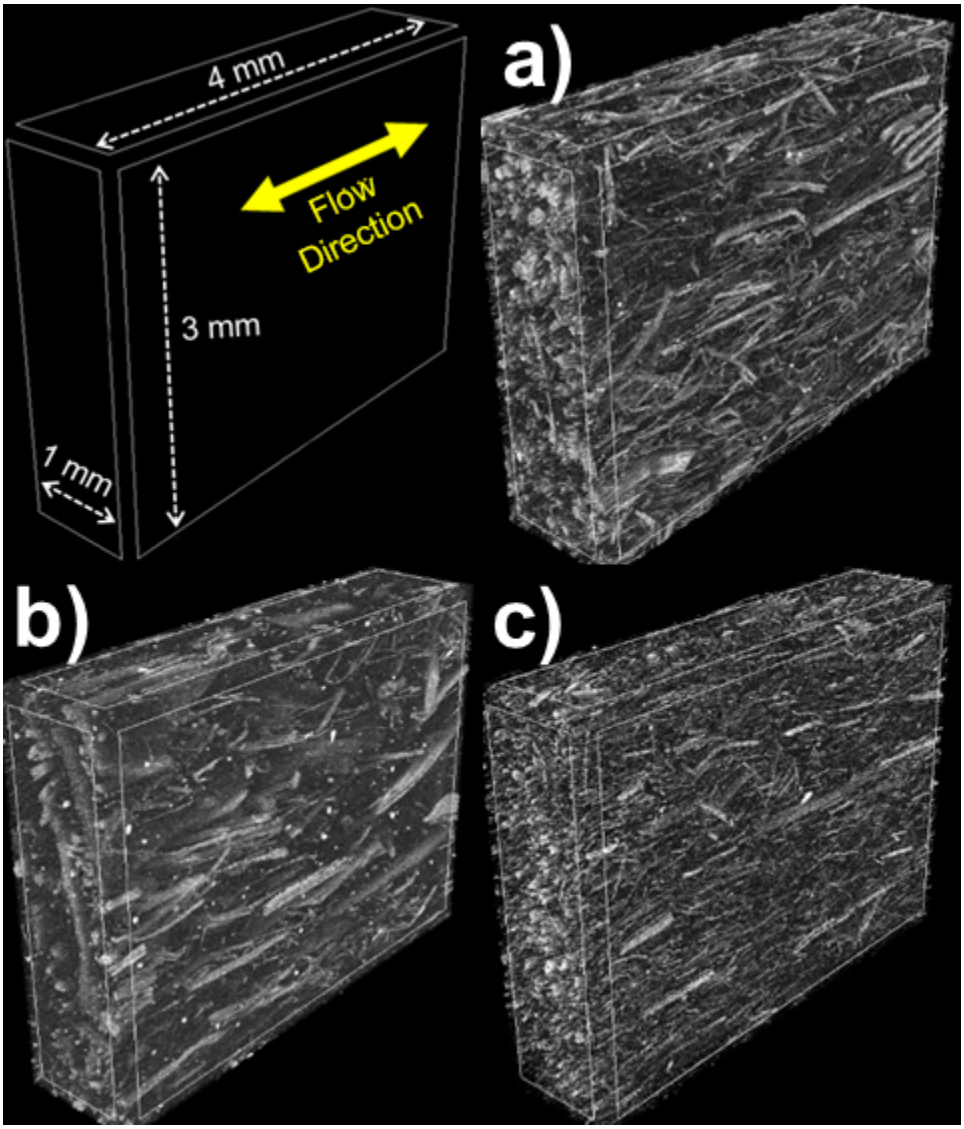

FIG. 8. Computer tomographs of injection-molded tensile test coupon sections (a) SSSPsc, (b) SSSPst and (c) SSSPft specimens.

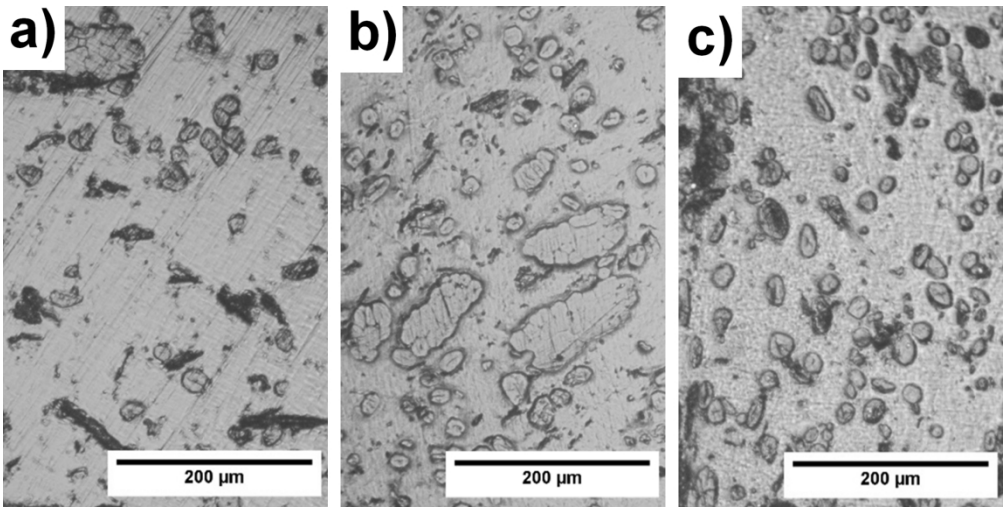

FIG. 9. Optical microscope images of polished surface of (a) SSSPsc, (b) SSSPst and (c) SSSPft specimens.

728x364mm (96 x 96 DPI)

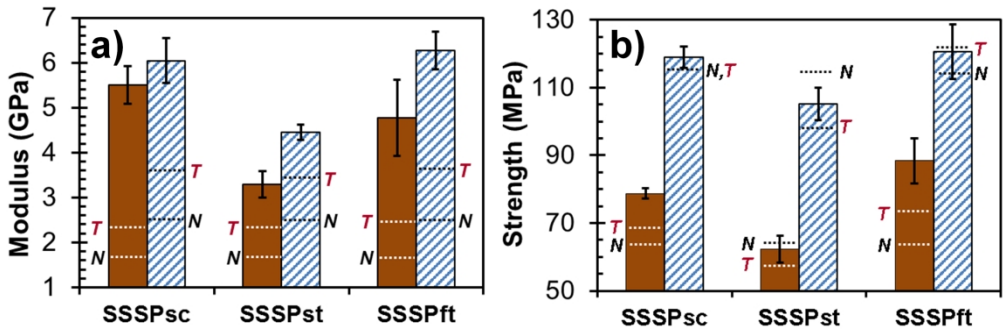

FIG. 10. Effect of flax type on (a) moduli and (b) strengths of PA6/ 20 wt% flax fiber composites, in tensile (solid) and flexural (stripes) modes. N and T benchmarks represent corresponding NEAT and TSE moduli and strengths, respectively. Error bars represent ± one standard deviation.

1019x333mm (96 x 96 DPI)